STATE ESTIMATION BASED ON STOCHASTIC AND ZONOTOPIC APPROACHES: PART II - NONLINEAR SYSTEMS

Alesi Augusto de Paula*, Guilherme Vianna Raffo*, Bruno Otávio Soares Teixeira*

* *Graduate Program in Electrical Engineering, Universidade Federal de Minas Gerais*
Av. Antônio Carlos 6627, 31270-901, Belo Horizonte, MG, Brazil

Emails: alesi@ufmg.br, raffo@ufmg.br, brunoot@ufmg.br

Resumo— Este artigo revisa de forma comparativa os métodos de filtragem estocástica e zonotópica bem conhecidos na literatura para estimação de estados de sistemas não lineares incertos. Para isso, uma notação unificada entre as abordagens é proposta. Enquanto o filtro de Kalman *unscented* provê de forma sub-ótima uma estimativa para a média por meio do critério de variância mínima e da transformação *unscented*, o filtro zonotópico busca garantir que os estados exatos de um dado sistema estejam contidos nos correspondentes conjuntos estimados. Dois exemplos numéricos ilustram os métodos revisitados.

Palavras-chave— Filtro de Kalman *unscented*, filtro zonotópico, estimação de estados, sistemas não lineares.

Abstract— This paper presents a comparative review on the well-known stochastic and zonotopic filtering methods in the literature for state estimation of uncertain nonlinear systems. To achieve that, a unified notation for both approaches is proposed. While the unscented Kalman filter provides a suboptimal estimate for the mean based on the minimum-variance criterion and the unscented transformation, the zonotopic filter seeks to guarantee that the true states of a given system are contained into the corresponding estimated sets. Two numerical examples illustrate the revisited methods.

Keywords— Unscented Kalman filter, zonotopic filter, state estimation, nonlinear systems.

1 Introduction

In 1960, it was introduced a method to estimate states of dynamical systems, the well-known Kalman filter (KF) (Kalman et al., 1960), which is optimal for linear systems with Gaussian noise. The KF presents basically two steps: *forecast* and *data-assimilation*. However, practical systems are nonlinear. Thereby, many variations of the KF have been proposed to estimate states of nonlinear systems such as the extended Kalman filter (EKF) and the unscented Kalman filter (UKF) (Särkkä, 2013).

The EKF linearizes the nonlinear model of the system by means of first-order truncated Taylor series, while the UKF is based on the unscented transformation (UT). The UT approximates the mean and covariance of the prior random variable (RV) by means of sigma points, which are deterministically chosen. In general, the UKF presents better performance than the EKF. Many variations have been developed based on the UKF, as the truncated UKF (Garcia-Fernandez et al., 2012) and the unscented Gaussian sum filter (Kottakki et al., 2014). Though these methods improve the state estimates, all nonlinear filters based on the stochastic approach provide approximate solutions.

The KF treats each state of a given system as a RV using usual statistical concepts (Kay, 1993). It is also possible to represent the same uncertain states by intervals, using interval arithmetic (Moore et al., 2009), or their derivations using affine arithmetic (Le et al., 2013).

Over the last decades, the set membership theory has owned relevance in the literature, since noise terms in a given system can be considered unknown but bounded (Alamo et al., 2005). Some usual compact sets are ellipsoids, polytopes, zonotopes, parallelotopes and boxes (Le et al., 2013). Therefore, filters that use the set membership approach treat the states and sources of uncertainty as compact sets. Some filters related to set membership for nonlinear cases are found in the literature. In (Alamo et al., 2005), the zonotopic filter (ZF) was proposed based on zonotopes and interval approximations with segment and volume minimization approaches. In (Alamo et al., 2008), an algorithm based on zonotopes and parallelotopes was proposed with difference of convex (DC) programming to bound the linearization error. In (Bo et al., 2013), an ellipsoidal algorithm was proposed based on linearizations and DC programming. Zonotopes are compact and centrally symmetric sets. Using Minkowski sum properties and affine transformations, a reduction in the computational burden is achieved.

This paper presents a comparison between the usual stochastic and zonotopic filtering methods in the literature for nonlinear cases, UKF and ZF respectively, exploring their advantages. The mean and the center estimates of the filters are compared by means of the performance index *root-mean-square error* (RMSE), while the corresponding uncertainty is analyzed graphically. Moreover, the performance index *mean processing time of CPU* (T^{CPU}) is evaluated for each algorithm. This is performed through a unified notation for both approaches. This paper is the nonlinear follow-up of (de Paula et al., 2018).

2 Background

Preliminary basic definitions and notations are introduced to characterize a Gaussian RV (GRV) and a zonotopic variable (ZV). Moreover, results for the nonlinear transformations of these variables are presented.

2.1 Nonlinear Transformations of Random Variables

A RV X is described by a probability density function (PDF) $p(x)$, where x is a realization of X, such that $x \in X$. The *mean* $\hat{x}$ of the RV X is defined as $\hat{x} = \mathrm{E}[X]$, where $\mathrm{E}[\bullet]$ is the *expected value* operator. The *covariance matrix* P^{xx} of a RV X is defined as

$$P^{\mathrm{xx}} = \mathrm{cov}(X) \triangleq \mathrm{E}\left[(X-\hat{x})(X-\hat{x})^{\mathrm{T}}\right].$$

In the case of a GRV X, its PDF is fully characterized by its mean $\hat{x}$ and covariance matrix P^{xx}. Moreover, for brevity, it is represented by $X \sim \mathcal{N}(\hat{x}, P^{\mathrm{xx}})$.

Let $Y = h(X_1, X_2, d)$ be a nonlinear transformation of the prior variables X_1 and X_2, and d a deterministic vector. Next, the steps of the UT are presented according to the systematization proposed by Menegaz et al. (2015).

Algorithm 2.1 *Unscented transformation.*
Let the general nonlinear transformation be

$$y = h(x_1, x_2, d), \tag{1}$$

where x_1 and x_2 are RVs with means $\hat{x}_1 \in \mathbb{R}^n$ and $\hat{x}_2 \in \mathbb{R}^r$ and covariances $P^{\mathrm{x_1x_1}} \in \mathbb{R}^{n\times n}$ and $P^{\mathrm{x_2x_2}} \in \mathbb{R}^{r\times r}$, and $d \in \mathbb{R}^p$ a deterministic vector.
1: Procedure

$$[\hat{y}, P^{\mathrm{yy}}, P^{\mathrm{x_1y}}] = \mathrm{UT}\left(\hat{x}_1, \hat{x}_2, P^{\mathrm{x_1x_1}}, P^{\mathrm{x_2x_2}}, d, h\right).$$

2: Given RVs x_1 and x_2, define the augmented state vector $\tilde{x} \in \mathbb{R}^{\tilde{n}}$

$$\tilde{x} \triangleq \begin{bmatrix} x_1 \\ x_2 \end{bmatrix}, \tag{2}$$

where $\tilde{n} = n + r$.
3: Based on matrices $P^{\mathrm{x_1x_1}}$ and $P^{\mathrm{x_2x_2}}$, define the augmented covariance matrix $P^{\tilde{\mathrm{x}}\tilde{\mathrm{x}}} \in \mathbb{R}^{\tilde{n}\times\tilde{n}}$

$$P^{\tilde{\mathrm{x}}\tilde{\mathrm{x}}} \triangleq \begin{bmatrix} P^{\mathrm{x_1x_1}} & 0_{n\times r} \\ 0_{r\times n} & P^{\mathrm{x_2x_2}} \end{bmatrix}. \tag{3}$$

4: Compute the sigma points $\mathrm{col}_j\left(X^{\mathrm{sp}}\right) \in \mathbb{R}^{\tilde{n}}$ and the corresponding weights $\gamma_j \in \mathbb{R}$, $j = 1, ..., 2\tilde{n}$,

$$\begin{aligned} X^{\mathrm{sp}} &\triangleq \begin{bmatrix} X^{\mathrm{sp1}} \\ X^{\mathrm{sp2}} \end{bmatrix} \\ &= \hat{\tilde{x}} 1_{1\times 2\tilde{n}} + \sqrt{\tilde{n}} \begin{bmatrix} \{\bullet\} & -\{\bullet\} \end{bmatrix}, \end{aligned} \tag{4}$$

$$\gamma_j = \frac{1}{2\tilde{n}}, \tag{5}$$

where $\{\bullet\} = \left(P^{\tilde{\mathrm{x}}\tilde{\mathrm{x}}}\right)^{1/2}$, $\mathrm{col}_j\left(X^{\mathrm{sp}}\right)$ is the j-th column of the matrix $X^{\mathrm{sp}} \in \mathbb{R}^{\tilde{n}\times 2\tilde{n}}$, $1_{1\times 2\tilde{n}} \in \mathbb{R}^{1\times 2\tilde{n}}$ is the vector of unitary elements, and $(\bullet)^{1/2}$ is the matrix square root. Moreover, $X^{\mathrm{sp1}} \in \mathbb{R}^{n\times 2\tilde{n}}$ and $X^{\mathrm{sp2}} \in \mathbb{R}^{r\times 2\tilde{n}}$ are partitions of the matrix X^{sp}.
5: Propagate each sigma point $\mathrm{col}_j\left(X^{\mathrm{sp1}}\right)$ and $\mathrm{col}_j\left(X^{\mathrm{sp2}}\right)$ by the transformation (1) generating

$$\mathrm{col}_j\left(Y^{\mathrm{sp}}\right) = h\left(\mathrm{col}_j\left(X^{\mathrm{sp1}}\right), \mathrm{col}_j\left(X^{\mathrm{sp2}}\right), d\right), \tag{6}$$

with $j = 1, ..., 2\tilde{n}$.
6: Finally, according to (6), estimate the mean $\hat{y}$ and the covariances P^{yy} and $P^{\mathrm{x_1y}}$

$$\hat{y} = \sum_{j=1}^{2\tilde{n}} \gamma_j \mathrm{col}_j\left(Y^{\mathrm{sp}}\right), \tag{7}$$

$$P^{\mathrm{yy}} = \sum_{j=1}^{2\tilde{n}} \gamma_j \left[\mathrm{col}_j\left(Y^{\mathrm{sp}}\right) - \hat{y}\right]\left[\mathrm{col}_j\left(Y^{\mathrm{sp}}\right) - \hat{y}\right]^{\mathrm{T}}, \tag{8}$$

$$P^{\mathrm{x_1y}} = \sum_{j=1}^{2\tilde{n}} \gamma_j \left[\mathrm{col}_j\left(X^{\mathrm{sp1}}\right) - \hat{x}_1\right]\left[\mathrm{col}_j\left(Y^{\mathrm{sp}}\right) - \hat{y}\right]^{\mathrm{T}}. \tag{9}$$

□

Fact 2.1 *(Julier and Uhlmann, 2004) Let $X_1 \sim \mathcal{N}(\hat{x}_1, P^{\mathrm{x_1x_1}})$ and $X_2 \sim \mathcal{N}(\hat{x}_2, P^{\mathrm{x_2x_2}})$ be GRVs. Applying the nonlinear transformation $Y = h(X_1, X_2, d)$ generates the RV Y whose mean $\hat{y}$ and covariance P^{yy} are approximated by*

$$[\hat{y}, P^{\mathrm{yy}}, P^{\mathrm{x_1y}}] = \mathrm{UT}\left(\hat{x}_1, \hat{x}_2, P^{\mathrm{x_1x_1}}, P^{\mathrm{x_2x_2}}, d, h\right). \tag{10}$$

2.2 Nonlinear Transformations of Zonotopic Variables

Set is a grouping of elements with similar characteristics, like ellipsoids, polytopes, intervals and zonotopes. An interval $[x] = [\underline{x}; \overline{x}]$ is the set $\{x \in \mathbb{R} : \underline{x} \leq x \leq \overline{x}\}$. The unitary interval is denoted as $[\Phi] = [-1; 1]$. A box is a n-dimensional interval vector defined as

$$[x] \triangleq \{x \in \mathbb{R}^n : \underline{x}_i \leq x_i \leq \overline{x}_i,\ i = 1, 2, ..., n\}.$$

The unitary box composed by n_g unitary intervals is denoted as $[\Phi]^{n_g}$. Given a box $[x]$, $\mathrm{mid}([x])_i \triangleq \dfrac{\underline{x}_i + \overline{x}_i}{2}$ is the i-th midpoint and $\mathrm{diam}([x])_i \triangleq \overline{x}_i - \underline{x}_i$ is the i-th diameter. The absolute value of the interval $[x]$ is given by $|[x]| \triangleq \max\{|\underline{x}|, |\overline{x}|\}$. The ∞-norm of the matrix $[A] \in \mathbb{R}^{n\times m}$ is defined as $||[A]||_\infty \triangleq \max_i \sum_j |[a_{i,j}]|$, for $i = 1, ..., n$ and $j = 1, ..., m$.

The four basic interval operations, namely, sum, subtraction, multiplication and division, are presented in (Moore et al., 2009). Thereby, it is possible to present the fundamental theorem of the interval arithmetic.

Theorem 2.1 *Natural interval extension (Alamo et al., 2005). Let $y = h(x)$ be a general nonlinear transformation, where $h : \mathbb{R}^n \to \mathbb{R}^m$ is a standard continuous function. Given an interval $[x]$, the*

natural interval extension function $\triangle\{h\}$ *is obtained substituting* x *by* $[x]$ *and all standard operations by corresponding interval operations, such that* $h([x]) \subseteq \triangle\{h\}([x])$*, where* $h([x])$ *is the exact transformation of* $[x]$*.*

Note that, due to Theorem 2.1, the natural interval extension is not unique. If an interval variable appears many times in the same expression, it may lead to an unnecessary overestimation called *dependency effect*. The following example shows a downside of using interval arithmetic.

Example 2.1 *Consider the equivalent standard functions* $h_1(x,y) = (x-y)^2$ *and* $h_2(x,y) = x^2 - 2xy + y^2$*. Given the intervals* $[x] = [1;3]$ *and* $[y] = [2;9]$*, the corresponding images are* $\triangle\{h_1\}([x],[y]) = [0;64]$ *and* $\triangle\{h_2\}([x],[y]) = [-49;86]$*. This is known as dependency effect.*

□

Another effect which can also generate unnecessary overestimation is called *wrapping effect*, which occurs when extra points are included in a given set by means of an overestimation (Moore et al., 2009).

Definition 2.1 *Minkowski sum (Alamo et al., 2005). The Minkowski sum of two sets is defined by the point-to-point sum*

$$\mathcal{X} \oplus \mathcal{Y} \triangleq \{x + y : x \in \mathcal{X}, y \in \mathcal{Y}\}.$$

The next fact allows to obtain a set less conservative than the natural interval extension does.

Fact 2.2 *Mean value extension (Alamo et al., 2005). Let* $h : \mathbb{R}^n \to \mathbb{R}^m$ *be a standard function, whose derivatives are continuous in* $\mathcal{X} \subset \mathbb{R}^n$*, and a real vector* $\hat{x} \in \mathcal{X}$*. Then,*

$$h(\mathcal{X}) \subseteq h(\hat{x}) \oplus \nabla_x h(\mathcal{X})(\mathcal{X} - \hat{x}), \tag{11}$$

where $\nabla_x h(\mathcal{X})$ *is the Jacobian matrix of* $h(x)$ *related to* x *and evaluated in* $\mathcal{X}$*.*

Definition 2.2 *Zonotope (Alamo et al., 2005). Given a vector* $\hat{x} \in \mathbb{R}^n$ *and a matrix* $G^{\mathrm{x}} \in \mathbb{R}^{n \times n_g}$*, a zonotope* $\mathcal{X}$ *of order* n_g *is defined as*

$$\hat{x} \oplus G^{\mathrm{x}}[\Phi]^{n_g} \triangleq \{\hat{x} + G^{\mathrm{x}}\xi : \xi \in [\Phi]^{n_g}, ||\xi||_\infty \leq 1\},$$

where $\hat{x}$ *and* G^{x} *are the center and generator matrix of the zonotope* $\mathcal{X}$*, respectively, and* $||\bullet||_\infty$ *is the* ∞*-norm of a vector.*

Thus, a ZV $\mathcal{X}$ is a variable whose values satisfy $x \in \mathcal{X}$. A width measure of zonotope can be given by the *Frobenius norm*, which is based on the 2-norm of each generator segment, that is, the column of the generator matrix G^{x}.

Definition 2.3 *Let* G^{x} *be the generator matrix of a zonotope such that* $G^{\mathrm{x}} = \begin{bmatrix} g_1^{\mathrm{x}} & g_2^{\mathrm{x}} & \cdots & g_{n_g}^{\mathrm{x}} \end{bmatrix}$*. The Frobenius norm of the generator matrix is defined as*

$$||G^{\mathrm{x}}||_{\mathrm{F}} \triangleq \sqrt{\sum_{j=1}^{n_g} \left|\left|g_j^{\mathrm{x}}\right|\right|_2^2}, \tag{12}$$

where $||\bullet||_2$ *is the 2-norm of a matrix.*

Analogously to Theorem 2.1, in the next result it is possible to compute a *zonotope inclusion* through the generalization of Kühn's method (Kühn, 1998).

Theorem 2.2 *Zonotope inclusion (Alamo et al., 2005). Consider a family of zonotopes represented by* $\mathcal{X} = \hat{x} \oplus [G^{\mathrm{x}}][\Phi]^{n_g}$*, where* $\hat{x} \in \mathbb{R}^n$ *is the center and* $[G^{\mathrm{x}}] \in \mathbb{R}^{n \times n_g}$ *is an interval generator matrix. A zonotope inclusion* $\diamond\{\mathcal{X}\}$ *is definided as*

$$\diamond\{\mathcal{X}\} \triangleq \hat{x} \oplus \begin{bmatrix} \mathrm{mid}([G^{\mathrm{x}}]) & L \end{bmatrix} \begin{bmatrix} [\Phi]^{n_g} \\ [\Phi]^n \end{bmatrix}, \tag{13}$$

where $L \in \mathbb{R}^{n \times n}$ *is a diagonal matrix whose elements are given by* $l_{i,i} = \sum_{j=1}^{n_g} \frac{\mathrm{diam}\left(\left[g_{i,j}^{\mathrm{x}}\right]\right)}{2}$*,* $i = 1, ..., n$*.*

It is common to reduce the order n_g of a zonotope $\mathcal{X}$ in order φ to obtain other one $\downarrow_\varphi \mathcal{X}$, but with the same center $\hat{x}$. This new zonotope is more conservative than the former, but it reduces the computational burden over operations. Given a desired order φ, the order reduction algorithm of a zonotope $\mathcal{X}$ is presented as follows.

Algorithm 2.2 *Zonotope order reduction (Le et al., 2013).*
1: Procedure $\downarrow_\varphi G^{\mathrm{x}} = \mathrm{red\_order}(G^{\mathrm{x}}, \varphi)$*.*
2: Calculate the 2-norm of each generator $g_j^{\mathrm{x}} = \mathrm{col}_j(G^{\mathrm{x}}) \in \mathbb{R}^n$ *of the matrix* G^{x} *and sort them in descending order:*

$$G^{\mathrm{xs}} = \begin{bmatrix} g_1^{\mathrm{x}} & ... & g_j^{\mathrm{x}} & ... & g_{n_g}^{\mathrm{x}} \end{bmatrix}, \tag{14}$$

where $\left|\left|g_j^{\mathrm{x}}\right|\right|_2 \geq \left|\left|g_{j+1}^{\mathrm{x}}\right|\right|_2$*.*
3: If $n_g \leq \varphi$*, then* $\downarrow_\varphi G^{\mathrm{x}} = G^{\mathrm{xs}}$*. Otherwise, given the sorted matrix* G^{xs}*, determine the matrices*

$$G_>^{\mathrm{x}} = \begin{bmatrix} g_1^{\mathrm{x}} & ... & g_{\varphi-n}^{\mathrm{x}} \end{bmatrix}, \tag{15}$$

which are the first $\varphi - n$ *columns of* G^{xs}*, and*

$$G_<^{\mathrm{x}} = \begin{bmatrix} g_{\varphi-n+1}^{\mathrm{x}} & ... & g_{n_g}^{\mathrm{x}} \end{bmatrix}, \tag{16}$$

which are the remaining columns of G^{xs}*.*
4: Calculate the matrix

$$G^{\mathrm{b}} = \mathrm{diag}\left(|G_<^{\mathrm{x}}|\, 1_{n_{g_<} \times 1}\right), \tag{17}$$

where $|G_<^{\mathrm{x}}|$ *is the absolute value of each element of the matrix* $G_<^{\mathrm{x}}$*,* $1_{n_{g_<} \times 1}$ *is the vector of unitary elements, and* $\mathrm{diag}(\bullet)$ *is the returned diagonal matrix.*
5: Finally, calculate the reduced generator matrix $\downarrow_\varphi G^{\mathrm{x}}$ *given by*

$$\downarrow_\varphi G^{\mathrm{x}} = \begin{bmatrix} G_>^{\mathrm{x}} & G^{\mathrm{b}} \end{bmatrix}. \tag{18}$$

□

Fact 2.3 *(Alamo et al., 2005) Let* $\mathcal{X}_1 = \hat{x}_1 \oplus G^{\mathrm{x}_1}[\Phi]^{n_g^{\mathrm{x}_1}} \subset \mathbb{R}^n$ *and* $\mathcal{X}_2 = \hat{x}_2 \oplus G^{\mathrm{x}_2}[\Phi]^{n_g^{\mathrm{x}_2}} \subset \mathbb{R}^r$ *be ZVs. Using the mean value extension (11), the nonlinear transformation* $\mathcal{Y} = h(\mathcal{X}_1, \mathcal{X}_2, d)$ *is overestimated by the zonotope*

$$\begin{aligned}\mathcal{Y} &= \hat{y} \oplus G^{\mathrm{y}}[\Phi]^{n_g^{\mathrm{y}}} \subset \mathbb{R}^m \\ &= \mathrm{mid}\left(h(\hat{x}_1, \mathcal{X}_2, d)\right) \oplus \begin{bmatrix} U & G^{\mathrm{i}} \end{bmatrix}[\Phi]^{n_g^{\mathrm{y}}}, \end{aligned} \tag{19}$$

where U *is the generator matrix of the set* $h(\hat{x}_1, \mathcal{X}_2, d)$*,* G^{i} *is the generator matrix of the inclusion zonotope* $\diamond\left\{0_{m\times 1} \oplus [M][\Phi]^{n_g^{\mathrm{x}_1}}\right\}$ *given by (13),* $[M] = \triangle\left\{\nabla_{x_1} h(\mathcal{X}_1, \mathcal{X}_2, d)\right\} G^{\mathrm{x}_1}$ *is the interval matrix and* $n_g^{\mathrm{y}} = n_g^{\mathrm{u}} + n + n_g^{\mathrm{x}_1}$*.*

3 Problem Formulation

Consider the discrete-time nonlinear dynamical system

$$x_k = f\left(x_{k-1}, w_{k-1}, u_{k-1}\right), \tag{20}$$
$$y_k = h\left(x_k, v_k\right), \tag{21}$$

where $f : \mathbb{R}^n \times \mathbb{R}^q \times \mathbb{R}^p \to \mathbb{R}^n$ and $h : \mathbb{R}^n \times \mathbb{R}^r \to \mathbb{R}^m$ are the process and measurement models, respectively, and $x_k \in \mathbb{R}^n$ is the state vector to be estimated. The variables w_{k-1} and v_k represent process and measurement noise terms, respectively. Since $k \geq 1$, the measurement vector $y_k \in \mathbb{R}^m$ and the input vector $u_{k-1} \in \mathbb{R}^p$ are assumed to be known. Two different assumptions can be made on the noise terms.

In the stochastic approach, the noise terms are white, Gaussian and uncorrelated, with zero mean and covariance matrices $\mathrm{E}\left[w_k w_k^{\mathrm{T}}\right] = Q_k$ and $\mathrm{E}\left[v_k v_k^{\mathrm{T}}\right] = R_k$. The estimates of the initial state $\hat{x}_0$ with covariance P_0^{xx} and the covariance matrices Q_{k-1} and R_k are assumed to be known.

In the zonotopic approach, the noise terms are unknown but bounded by the corresponding zonotopes $w_{k-1} \in \mathcal{W}_{k-1}$ and $v_k \in \mathcal{V}_k$. The initial states must satisfy the zonotopic set $x_0 \in \mathcal{X}_0$. The sets $\mathcal{W}_{k-1} = \hat{w}_{k-1} \oplus G_{k-1}^{\mathrm{w}}[\Phi]^{n_g^{\mathrm{w}}}$, $\mathcal{V}_k = \hat{v}_k \oplus G_k^{\mathrm{v}}[\Phi]^{n_g^{\mathrm{v}}}$ and $\mathcal{X}_0 = \hat{x}_0 \oplus G_0^{\mathrm{x}}[\Phi]^{n_g^{\mathrm{x}}}$ are known.

4 Nonlinear State Estimators

The UKF and the ZF basically use the process model to obtain the *a priori* estimates. After, this information is used with the measurement model to calculate the transformed estimates, which are consistent with the measurements. Finally, each estimate is weighted by an uncertainty reduction criterion to obtain the *a posteriori* estimates.

4.1 Unscented Kalman Filter

First, determine the *a priori* estimates $X_{k|k-1} \sim \mathcal{N}\left(\hat{x}_{k|k-1}, P_{k|k-1}^{\mathrm{xx}}\right)$ by

$$\left[\hat{x}_{k|k-1}, P_{k|k-1}^{\mathrm{xx}}, P_{k|k-1}^{\mathrm{c}}\right] = \mathrm{UT}\left(\hat{x}_{k-1}, 0_{q\times 1}, P_{k-1}^{\mathrm{xx}}, Q_{k-1}, u_{k-1}, f\right), \tag{22}$$

where $P_{k|k-1}^{\mathrm{c}} = \mathrm{cov}\left(X_{k-1}, X_{k|k-1}\right)$.

After, determine the transformed estimates of mean $\hat{y}_{k|k-1}$ and covariances $P_{k|k-1}^{\mathrm{yy}}$ and $P_{k|k-1}^{\mathrm{xy}}$ by

$$\left[\hat{y}_{k|k-1}, P_{k|k-1}^{\mathrm{yy}}, P_{k|k-1}^{\mathrm{xy}}\right] = \mathrm{UT}\left(\hat{x}_{k|k-1}, 0_{r\times 1}, P_{k|k-1}^{\mathrm{xx}}, R_k, 0, h\right). \tag{23}$$

These proceedings compound the forecast step.

The data-assimilation step is the same of the KF, where the Kalman gain

$$K_k = P_{k|k-1}^{\mathrm{xy}}\left(P_{k|k-1}^{\mathrm{yy}}\right)^{-1} \tag{24}$$

is used to calculate the *a posteriori* estimates $X_k \sim \mathcal{N}\left(\hat{x}_k, P_k^{\mathrm{xx}}\right)$

$$\hat{x}_k = \hat{x}_{k|k-1} + K_k\left(y_k - \hat{y}_{k|k-1}\right), \tag{25}$$
$$P_k^{\mathrm{xx}} = P_{k|k-1}^{\mathrm{xx}} - K_k P_{k|k-1}^{\mathrm{yy}} K_k^{\mathrm{T}}. \tag{26}$$

4.2 Zonotopic Filter

This algorithm is presented for the non-autonomous case (Rego and Raffo, 2016), with two types of minimization, namely: segment minimization, proposed by Alamo et al. (2005), and volume minimization, proposed by Bravo et al. (2006). Like the UKF algorithm, the ZF algorithm uses information related to the system (20)-(21) and the measurements y_k to determine the predicted and consistent state sets. Through an intersection between these sets subject to any minimization criterion, the final zonotope incorporates information related to both system model and measurements. Finally, this zonotope is reduced based on the order φ.

At first, given the process model (20), the zonotope $\mathcal{X}_{k-1} = \hat{x}_{k-1} \oplus G_{k-1}^{\mathrm{x}}[\Phi]^{n_g^{\mathrm{x}}}$ and the zonotope $\mathcal{W}_{k-1} = \hat{w}_{k-1} \oplus G_{k-1}^{\mathrm{w}}[\Phi]^{n_g^{\mathrm{w}}}$, determine the zonotope

$$\mathcal{Z} \triangleq f\left(\hat{x}_{k-1}, \mathcal{W}_{k-1}, u_{k-1}\right), \tag{27}$$

the interval matrix

$$[M] \triangleq \triangle\left\{\nabla_x f\left(\mathcal{X}_{k-1}, \mathcal{W}_{k-1}, u_{k-1}\right)\right\} G_{k-1}^{\mathrm{x}}, \tag{28}$$

and, then, the predicted zonotope is given by

$$\mathcal{X}_{k|k-1} = \mathcal{Z} \oplus \diamond\left\{0_{n\times 1} \oplus [M][\Phi]^{n_g^{\mathrm{x}}}\right\}. \tag{29}$$

Next, given the zonotope $\mathcal{V}_k = \hat{v}_k \oplus G_k^{\mathrm{v}}[\Phi]^{n_g^{\mathrm{v}}}$ and the measurement model (21), obtain through

interval arithmetic the vector c_i and the scalars $s_i,\ \rho_i \in \mathbb{R}$

$$c_i = \text{mid}\left(\triangle\left\{\ \nabla_x h_i\left(\mathcal{X}_{k|k-1}, \mathcal{V}_k\right)^{\mathrm{T}}\ \right\}\right), \tag{30}$$

$$[\Lambda] = \triangle\left\{c_i^{\mathrm{T}}\mathcal{X}^{\mathrm{x}}_{k|k-1} - h_i\left(\mathcal{X}^{\mathrm{x}}_{k|k-1}, \mathcal{X}^{\mathrm{v}}_{k}\right)\right\}, \tag{31}$$

$$s_i = \text{mid}([\Lambda]) \in \mathbb{R}, \tag{32}$$

$$\rho_i = \frac{1}{2}\text{diam}([\Lambda]) \in \mathbb{R}. \tag{33}$$

Based on c_i, the i-th measurement $y_{i,k}$ and the scalars s_i and ρ_i, a strip $\mathcal{Y}_{i,k|k-1} = \left\{x \in \mathbb{R}^n : \left|c_i^{\mathrm{T}}x - d_i\right| \leq \rho_i\right\}$ is defined, where $d_i = y_{i,k} + s_i$.

After, calculate the intersection $\mathcal{X}_k$ between the predicted zonotope $\mathcal{X}_{k|k-1} = \hat{x}_{k|k-1} \oplus \begin{bmatrix} g_1^{\mathrm{x}} & g_2^{\mathrm{x}} & \dots & g_{n_g}^{\mathrm{x}}\end{bmatrix}[\Phi]^{n_g}$ and the strip $\mathcal{Y}_{k|k-1} = \left\{x \in \mathbb{R}^n : \left|c^{\mathrm{T}}x - d\right| \leq \rho\right\}$. In this paper, two criteria are presented to do intersection, namely: volume minimization and segment minimization.

In the volume minimization, $(n_g + 1)$ zonotopes $\bar{\mathcal{X}}(j) = \bar{x}(j) \oplus \bar{G}(j)[\Phi]^{n_g}$ are defined, for $j = 0, 1, ..., n_g$, as the intersection between $\mathcal{X}_{k|k-1}$ and $\mathcal{Y}_{k|k-1}$, where

$$\bar{x}(j) = \begin{cases} \hat{x}_{k|k-1} + \frac{\left(d - c^{\mathrm{T}}\hat{x}_{k|k-1}\right)}{c^{\mathrm{T}}g_j^{\mathrm{x}}}g_j^{\mathrm{x}}, & \text{if } 1 \leq j \leq n_g \\ & \text{and } c^{\mathrm{T}}g_j^{\mathrm{x}} \neq 0 \\ \hat{x}_{k|k-1}, & \text{otherwise,} \end{cases} \tag{34}$$

$$\bar{g}_i^j = \begin{cases} g_i^{\mathrm{x}} - \frac{c^{\mathrm{T}}g_i^{\mathrm{x}}}{c^{\mathrm{T}}g_j^{\mathrm{x}}}g_j^{\mathrm{x}}, & \text{if } i \neq j \\ \frac{\rho}{c^{\mathrm{T}}g_j^{\mathrm{x}}}g_j^{\mathrm{x}}, & \text{if } i = j, \end{cases} \tag{35}$$

$$\bar{G}(j) = \begin{cases} \begin{bmatrix}\bar{g}_1^j & \bar{g}_2^j & ... & \bar{g}_{n_g}^j\end{bmatrix}, & \text{if } 1 \leq j \leq n_g \\ & \text{and } c^{\mathrm{T}}g_j^{\mathrm{x}} \neq 0 \\ G^{\mathrm{x}}, & \text{otherwise.} \end{cases} \tag{36}$$

The chosen zonotope is the one with the smallest volume based on the zonotope volume equation

$$\text{Vol}\left(\bar{\mathcal{X}}\right) = 2^n \sum_{i=1}^{N\left(n_g, n\right)} \left|\det(T_i)\right|, \tag{37}$$

where $N\left(n_g, n\right)$ is the mathematical combination that returns all possible ways to choose n elements of a set n_g, and $T_i \in \mathbb{R}^{n\times n}$ denotes all matrices that can be obtained taking n columns of the matrix $\bar{G}$.

If there are more than one measurement, that is, $m > 1$, this zonotope is used to define another strip and a new intersection is performed with all of them, until all measurements $y_{i,k}$, $i = 1, ..., m$, are used.

Finally, given the desired order φ, use Algorithm 2.2 on the zonotope $\bar{\mathcal{X}}$ to obtain $\downarrow_\varphi G_k^{\mathrm{x}} = \text{red\_order}(\bar{G}, \varphi)$.

Alternatively, another criterion to compute the intersection $\mathcal{X}_k$ is to minimize the Frobenius norm of its generator matrix, called segment minimization. This criterion is used when it is necessary to reduce computational burden. According to the predicted zonotope $\mathcal{X}_{k|k-1}$ and the strip $\mathcal{Y}_{k|k-1}$, compute the vector $\lambda \in \mathbb{R}^n$

$$\lambda = \frac{G^{\mathrm{x}}_{k|k-1}\left(G^{\mathrm{x}}_{k|k-1}\right)^{\mathrm{T}}c}{c^{\mathrm{T}}G^{\mathrm{x}}_{k|k-1}\left(G^{\mathrm{x}}_{k|k-1}\right)^{\mathrm{T}}c + \rho^2}. \tag{38}$$

Thus, the intersection $\mathcal{X}_k$ is given by

$$\hat{x}_k = \hat{x}_{k|k-1} + \lambda\left(d - c^{\mathrm{T}}\hat{x}_{k|k-1}\right), \tag{39}$$

$$G_k^{\mathrm{x}} = \begin{bmatrix}\left(I_{n\times n} - \lambda c^{\mathrm{T}}\right)G^{\mathrm{x}}_{k|k-1} & \rho\lambda\end{bmatrix}. \tag{40}$$

When the measurement model is nonlinear, the computed strip has varying width due to the dependency effect. Therefore, the ZF can diverge. To circumvent this, the system is linearized as

$$\begin{aligned} x_k =& f(x^{\mathrm{eq}}, w^{\mathrm{eq}}, u^{\mathrm{eq}}) + \nabla_x f(x^{\mathrm{eq}}, w^{\mathrm{eq}}, u^{\mathrm{eq}})(x_{k-1} - x^{\mathrm{eq}}) \\ &+ \nabla_u f(x^{\mathrm{eq}}, w^{\mathrm{eq}}, u^{\mathrm{eq}})(u_{k-1} - u^{\mathrm{eq}}) + \nabla_w f(x^{\mathrm{eq}}, w^{\mathrm{eq}}, u^{\mathrm{eq}})\bar{w}_{k-1}, \end{aligned} \tag{41}$$

$$y_k = h(x^{\mathrm{eq}}, v^{\mathrm{eq}}) + \nabla_x h(x^{\mathrm{eq}}, v^{\mathrm{eq}})(x_k - x^{\mathrm{eq}}) + \nabla_v h(x^{\mathrm{eq}}, v^{\mathrm{eq}})\bar{v}_k, \tag{42}$$

where the noise terms $\bar{w}_{k-1}$ and $\bar{v}_k$ represent disturbances and errors of linearization at the same time. This linearization takes into account the correction of the equilibrium points $w^{\mathrm{eq}} = 0_{q\times 1}$ and $v^{\mathrm{eq}} = 0_{r\times 1}$, being x^{eq} set as the most current center of the zonotope $\mathcal{X}$. Therefore, note that (30)-(31) are rewritten as

$$c_i = \nabla_x h_i\left(x^{\mathrm{eq}}, v^{\mathrm{eq}}\right)^{\mathrm{T}}, \tag{43}$$

$$[\Lambda] = \nabla_x h_i\left(x^{\mathrm{eq}}, v^{\mathrm{eq}}\right)x^{\mathrm{eq}} - h_i\left(x^{\mathrm{eq}}, v^{\mathrm{eq}}\right) - \mathcal{V}_{i,k}. \tag{44}$$

5 Numerical Examples

5.1 Batch Reactor

5.1.1 Process Description

The reversible gas-phase reaction in a batch reactor is considered (Alamo et al., 2005) $2\mathrm{R}^{\mathrm{A}} \underset{k_2}{\overset{k_1}{\rightleftharpoons}} \mathrm{R}^{\mathrm{B}}$, where $k_1 = 0.16\text{min}^{-1}\text{atm}^{-1}$ and $k_2 = 0.0064\text{min}^{-1}$. The reactions occur in isothermal and constant volume conditions. Defining the state vector $x(t) \in \mathbb{R}^2_+$ as the partial pressures of $\mathrm{R_A}$ and $\mathrm{R_B}$ in atm, the system is modeled by

$$\begin{bmatrix}\dot{x}_1(t) \\ \dot{x}_2(t)\end{bmatrix} = \begin{bmatrix}-2k_1x_1^2(t) + 2k_2x_2(t) \\ k_1x_1^2(t) - k_2x_2(t)\end{bmatrix}. \tag{45}$$

It is considered that the output pressure is measured

$$y_k = \begin{bmatrix}1 & 1\end{bmatrix}x_k + v_k, \tag{46}$$

where $v_k \in V_k$ is the measurement noise.

The system is simulated with $x_0 = \begin{bmatrix}3 & 1\end{bmatrix}^{\mathrm{T}}$ using the sampling time $T_{\mathrm{s}} = 1\text{s}$, and a fixed step fourth-order Runge Kutta integration to discretize the continuous dynamics. No process noise is added on the states. The noise realizations v_k are such that $V_k \sim \mathcal{N}(0, 0.01)$. To estimate the

states, the UKF and the ZF are used. The parameters of the UKF are set as $\hat{x}_0 = \begin{bmatrix}2.5 & 1.5\end{bmatrix}^{\mathrm{T}}$ with covariance $P_0^{\mathrm{xx}} = 0.16 I_{2\times 2}$, and the covariance matrices $Q_{k-1} = 10^{-10} I_{2\times 2}$ and $R_k = 0.01$. Although there is no process noise, the covariance matrix Q_{k-1} is added to improve the convergence of the UKF.
The parameters of the ZF are set as $\mathcal{X}_0 = \hat{x}_0 \oplus 1.2 I_{2\times 2}[\Phi]^2$, $\mathcal{W}_{k-1} = 0_{2\times 1} \oplus 3 \times 10^{-5} I_{2\times 2}[\Phi]^2$, $\mathcal{V}_k = 0 \oplus 0.3[\Phi]$ and order reduction $\varphi = 14$, such that each interval contains the corresponding uncertainty with confidence level 99.73%. In this case, the ZF is used with the volume minimization.
The states estimated by each filter are compared through the *root-mean-square error* of the j-th state (RMSE_j)

$$\mathrm{RMSE}_j = \frac{1}{100}\sum_{m=1}^{100}\sqrt{\frac{1}{N}\sum_{k=1}^{N}(x_{j,k} - \hat{x}_{j,k,m})^2}, \quad (47)$$

where $j = 1, ..., n$, is the j-th element of the state vector, N is the final time step, and m is the m-th Monte Carlo realization.
Moreover, the mean processing time of CPU (T^{CPU}) is used to compare the algorithms. The used computer configuration is: HD 160Gb, RAM memory 3.25Gb, Windows 7 Ultimate, Intel core 2 Quad CPU Q6700 2.66GHz and off-board video card Geforce 9600Gt 512Mb.

5.1.2 State Estimation

The tuning of states and noise terms is in the convergence threshold of the ZF, that is, for larger values there is some realization where the ZF diverges. Figure 1 corresponds to a Monte Carlo realization of the state estimation for the batch reactor. Due to the ZF using the worst case of noise tuning as 3σ of the uncertainties related to the UKF, its interval is larger than the confidence level $3\sigma_x$. However, as the ZF sometimes fails to include the true state x_2 around 1350s, it evidences that some assumption on bounded noise terms has been violated. Furthermore, the ZF with the volume minimization is more sensitive to linearization errors, since the state estimation x_2 presents amplitude fast transitions.

Due to sensitivity to initial conditions, the ZF can diverge when the Jacobian matrix is subject to the wrapping effect, while the UKF does not diverge but retards its convergence. Although the initial conditions are well tuned, as the segment minimization does not reduce effectively volume, the ZF can become sensitive to nonlinear dynamics and diverge.

Based on the index RMSE after 100 Monte Carlo realizations in Table 1, it is verified that the estimated means are more accurate than the estimated centers. It occurs due to the confidence level being more accurate than the interval. The index T^{CPU} for UKF and ZF is 1.5μs and 40μs, respectively. These values are smaller than the sampling time $T_{\mathrm{s}} = 1$s, allowing practical application of these algorithms.

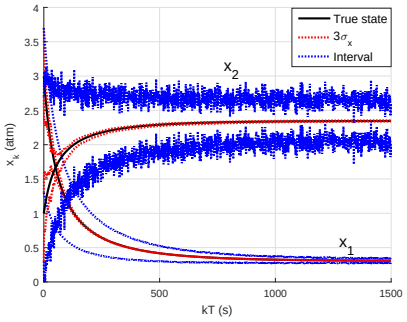

Figure 1: State estimation of the batch reactor for one Monte Carlo realization. The black solid lines are the true states of the system, the red and blue solid lines are, respectively, the estimated means and centers, and the dotted lines are their corresponding uncertainty, the usual confidence level $3\sigma_{x_{i,k}} \triangleq 3\sqrt{P^{\mathrm{xx}}_{(i,i),k}}$ for $i = 1, 2$ and the interval $\triangle\{\mathcal{X}_k\}$.

Table 1: RMSE of estimated means and centers for the batch reactor after 100 Monte Carlo realizations.

	UKF	ZF
$\hat{x}_1(10^{-2}\mathrm{atm})$	1.11	3.63
$\hat{x}_2(10^{-2}\mathrm{atm})$	1.62	10.3

5.2 Tracking a Ground Vehicle

5.2.1 Process Description

Consider the vehicle tracking problem presented in (Xu et al., 2017), whose nonlinear process model is modified to

$$x_k = \begin{bmatrix} x_{1,k-1} + T_{\mathrm{s}} x_{3,k-1} \\ x_{2,k-1} + T_{\mathrm{s}} x_{4,k-1} \\ x_{3,k-1} s/s_k^{\mathrm{a}} \\ x_{4,k-1} s/s_k^{\mathrm{a}} \end{bmatrix} + w_{k-1}, \quad (48)$$

where $T_{\mathrm{s}} = 0.5$s is the sampling time, $s = 15$m/s is the reference constant speed and $s_k^{\mathrm{a}} = \sqrt{x_{3,k-1}^2 + x_{4,k-1}^2}$ is the normalization term of the speed components such that

$$x_{3,k}^2 + x_{4,k}^2 = s^2. \quad (49)$$

The process noise term $w_{k-1} \sim \mathcal{N}(0_{4\times 1}, Q_{k-1})$ is white with covariance

$$Q_{k-1} = \left(\begin{bmatrix}0 & 0 & 0.01 & 0.01\end{bmatrix}^{\mathrm{T}}\right), \quad (50)$$

and with standard deviation σ_w, such that $\sigma_{w_{3,4}} = 0.1$m/s is considered an accurate error for the speed states.

The position of this vehicle is assumed to be measured in polar coordinates on the plane $\mathbb{R}^2$ and is given by the measurement model

$$y_k = \begin{bmatrix} \sqrt{x_{1,k}^2 + x_{2,k}^2} \\ \text{atan}\left(\frac{x_{2,k}}{x_{1,k}}\right) \end{bmatrix} + v_k, \tag{51}$$

where $v_k \sim \mathcal{N}(0_{2\times 1}, R_k)$ is the measurement noise term with standard deviation σ_v such that $3\sigma_{v_1} = 0.15$m and $3\sigma_{v_2} = 2.618 \times 10^{-3}$rad, which are given by accurate sensors, GPS NovAtel OEMStar and IMU Xsens MTi-G respectively (Rego and Raffo, 2016).
This system is simulated with $x_0 = \begin{bmatrix}5 & 5 & 1 & 1\end{bmatrix}^{\mathrm{T}}$. To estimate the states using UKF, the parameters are set as $\hat{x}_0 = \begin{bmatrix}3 & 3 & 3 & 3\end{bmatrix}^{\mathrm{T}}$ and covariance matrices $P_0^{\mathrm{xx}} = I_{4\times 4}$, $\bar{Q}_{k-1} = 1.5Q_{k-1}$ and $\bar{R}_k = 1.5R_k$, which represent the effective noise terms, including errors of statistical linearization. The terms $\bar{Q}$ and $\bar{R}$ are set based on the minimal noise tuning such that the UKF can include the true states.
To estimate the states using the ZF, all system is linearized with x^{eq} set as the center of the most current zonotope $\mathcal{X}$, since the measurement model (51) is nonlinear. The parameters are set as $\mathcal{X}_0 = \hat{x}_0 \oplus 3I_{4\times 4}[\Phi]^4$, $\mathcal{W}_{k-1} = 0_{4\times 1} \oplus \text{diag}\left(\begin{bmatrix}0 & 0 & 0.3674 & 0.3674\end{bmatrix}^{\mathrm{T}}\right)[\Phi]^4$ and $\mathcal{V}_k = 0_{2\times 1} \oplus 10^{-2}\text{diag}\left(\begin{bmatrix}18.37 & 0.32\end{bmatrix}^{\mathrm{T}}\right)[\Phi]^2$. The noise tuning for the ZF is set as the minimal boxes that contain the noise tuning for the UKF with 3σ. To reduce the uncertainty of the estimated zonotope, the order reduction φ is set as $\varphi = 10,000$, being impracticable to use the volume minimization. Then, the ZF is used with the segment minimization, since this approach is faster.

5.2.2 State Estimation

As all system is nonlinear, linearization errors are more expressive than those in the prior example. Then, it is necessary to consider errors larger than those effectively present in the nonlinear system. The ZF with volume minimization generates results more accurate (not shown) than the segment minimization does, but its index T^{CPU} is larger than 0.5s, since many candidate zonotopes and their volume are computed, and the uncertainty varies fastly the order of magnitude, since the linearization errors are dynamic and can lead to zonotopes with much different volumes over time. Using the nonlinear system to estimate states with ZF does not guarantee convergence, due to wrapping and dependency effects in the prediction step, and dependency effect in the measurement step.

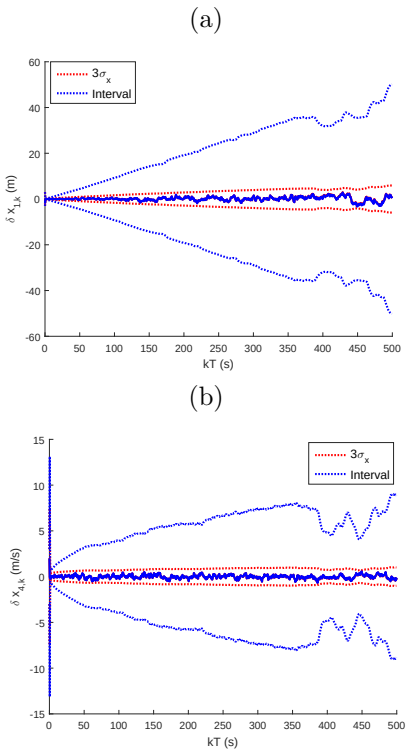

Figure 2: State estimation of the vehicle tracking system. (a)-(b) present the error results related to the position and speed states, x_1 and x_4 respectively, for one Monte Carlo realization. The red and blue solid lines are the estimated means and centers, respectively, and the dotted lines are their uncertainties, confidence level $3\sigma_{x_k}$ and interval $\triangle\{\mathcal{X}_k\}$.

In Figure 2, the state estimation errors for x_1 and x_4 are presented for one Monte Carlo realization. The results related to the remaining states are omitted, because they are similar to the corresponding states. Note that the integrating feature of the position states is transferred for the speed states. This is the reason why the error of each state increases over time. Moreover, the interval generated by the ZF is more conservative than the usual $3\sigma_x$ of the UKF. This occurs due to two factors: (i) the design tuning of the ZF being more conservative, which is an alternative to lead to guaranteed estimation, and (ii) the segment minimization, since this approach does not reduce volume effectively.

Table 2: RMSE of estimated means and centers for the tracking system after 100 Monte Carlo realizations.

	$\hat{x}_1$(m)	$\hat{x}_2$(m)	$\hat{x}_3$(m/s)	$\hat{x}_4$(m/s)
UKF/ZF	0.87	0.87	0.22	0.22

Based on the RMSE of each estimated state after 100 Monte Carlo realizations in Table 2, it is verified that the estimated centers are as accurate as the estimated means due to three factors:

(i) the noise terms are accurate, (ii) the segment minimization reduces 2-norm and (iii) there are no wrapping and dependency effects. It shows the estimated means are not always more accurate than the estimated centers. The index T^{CPU} for UKF and ZF is 0.226ms and 27.2ms, respectively, which are smaller than the sampling time $T_{\text{s}} = 0.5$s, allowing practical application. In this case, T^{CPU} for ZF is much larger due to zonotope order increasing over time.

6 Conclusions

This paper compared the estimated mean to the estimated center and the corresponding uncertainty related to each filter, namely, covariance and generator matrices. On one hand, the main advantage of the UKF is the accuracy of the mean and the uncertainty due to the measurement sequence and the Kalman gain, that performs the minimum-variance sub-optimal criterion. On other hand, the main disadvantage is to generate approximated estimates, which can fail to include the true states, since nonlinearity does not preserve the Gaussian feature. In general, the UKF is sensitive to initial conditions, but it does not diverge, since the poor tuning retards the convergence. The ZF is an algorithm based on numerical approximations and it allows estimate guaranteed state sets when the performed assumptions on initial states and noise terms are satisfied. This is the main advantage of the ZF. The accuracy of its uncertainty depends on the number of generators, which defines in practice what minimization criterion is applicable, namely, segment or volume. The first one generates results faster while the second one generates more accurate results taking much time. Then, computational burden is a disadvantage. Specially for nonlinear cases, the ZF is sensitive to initial conditions and it can diverge due to the interval arithmetic being used. In general, divergence can be observed in ZF when: (i) process model is nonlinear, due to the wrapping and/or dependency effects, and (ii) measurement model is nonlinear, due to the dependency effect. Moreover, the segment minimization gives to the ZF sensitivity to nonlinear systems, but the volume minimization is not enough to guarantee neither convergence for any nonlinear system nor the same accuracy for each state.

Acknowledgments

This work has been supported by the Brazilian agencies CAPES, FAPEMIG and CNPq.

References

Alamo, T., Bravo, J. M. and Camacho, E. F. (2005). Guaranteed state estimation by Zonotopes, *Automatica* **41**(6): 1035–1043.

Alamo, T., Bravo, J. M., Redondo, M. and Camacho, E. F. (2008). A set-membership state estimation algorithm based on DC programming, *Automatica* **44**(1): 216–224.

Bo, Z., Kun, Q., Xu-Dong, M. and Xian-Zhong, D. (2013). A new nonlinear set membership filter based on guaranteed bounding ellipsoid algorithm, *Acta Automatica Sinica* **39**(2): 146–154.

Bravo, J. M., Alamo, T. and Camacho, E. F. (2006). Bounded error identification of systems with time-varying parameters, *IEEE Transactions on Automatic Control* **51**(7): 1144–1150.

de Paula, A. A., Raffo, G. V. and Teixeira, B. O. (2018). State estimation for uncertain linear systems: a comparative analysis between stochastic and zonotopic approaches, *XXII Congresso Brasileiro de Automática, 2018, João Pessoa*, Anais do XXII Congresso Brasileiro de Automática, pp. 1–6. Submitted.

Garcia-Fernandez, Á. F., Morelande, M. R. and Grajal, J. (2012). Truncated unscented Kalman filtering, *IEEE Transactions on Signal Processing* **60**(7): 3372–3386.

Julier, S. J. and Uhlmann, J. K. (2004). Unscented filtering and nonlinear estimation, *Proceedings of the IEEE* **92**(3): 401–422.

Kalman, R. E. et al. (1960). A new approach to linear filtering and prediction problems, *Journal of basic Engineering* **82**(1): 35–45.

Kay, S. M. (1993). *Fundamentals of statistical signal processing*, Prentice Hall PTR.

Kottakki, K. K., Bhushan, M. and Bhartiya, S. (2014). Interval constrained state estimation of nonlinear dynamical systems using unscented Gaussian sum filter, *Control Conference (AUCC), 2014 4th Australian*, IEEE, pp. 297–302.

Kühn, W. (1998). Rigorously computed orbits of dynamical systems without the wrapping effect, *Computing* **61**(1): 47–67.

Le, V. T. H., Stoica, C., Alamo, T., Camacho, E. F. and Dumur, D. (2013). *Zonotopes: From guaranteed state-estimation to control*, John Wiley & Sons.

Menegaz, H. M., Ishihara, J. Y., Borges, G. A. and Vargas, A. N. (2015). A systematization of the unscented Kalman filter theory, *IEEE Transactions on Automatic Control* **60**(10): 2583–2598.

Moore, R. E., Kearfott, R. B. and Cloud, M. J. (2009). *Introduction to interval analysis*, SIAM.

Rego, B. S. and Raffo, G. V. (2016). Suspended load path tracking control based on zonotopic state estimation using a tilt-rotor UAV, *Intelligent Transportation Systems (ITSC), 2016 IEEE 19th International Conference on*, IEEE, pp. 1445–1451.

Särkkä, S. (2013). *Bayesian filtering and smoothing*, Vol. 3, Cambridge University Press.

Xu, L., Li, X. R., Liang, Y. and Duan, Z. (2017). Constrained dynamic systems: Generalized modeling and state estimation, *IEEE Transactions on Aerospace and Electronic Systems* **53**(5): 2594–2609.